




PAPER

View Article Online
View Journal



Cite this: DOI: 10.1039/d0en00574f

Copper oxide nanoparticle dissolution at alkaline pH is controlled by dissolved organic matter: influence of soil-derived organic matter, wheat, bacteria, and nanoparticle coating†

J. M. Hortin, ^a A. J. Anderson, ^b D. W. Britt, ^b
A. R. Jacobson^c and J. E. McLean^{*a}

Dissolution of CuO nanoparticles, releasing Cu ions, is a primary mechanism of Cu interaction in the rooting zone of plants. CuO dissolution is sometimes incorrectly considered negligible at high pH, since complexation of Cu with dissolved organic matter may enhance nanoparticle dissolution. Therefore data on the effects of plant-microbial-soil interactions on nanoparticle dissolution, particularly in alkaline soils, are needed. Dissolution of CuO nanoparticles (100 mg kg⁻¹ Cu) was studied in sand supplemented with factorial combinations of wheat growth, a root-colonizing bacterium, and saturated paste extracts (SPEs) from three alkaline, calcareous soils. In control sand systems with 3.34 mM Ca(NO₃)₂ solution, dissolved Cu was low (266 µg L⁻¹ Cu). Addition of dissolved organic matter via wheat root metabolites and/or soil SPEs increased dissolved Cu to 795–6250 µg L⁻¹ Cu. Dissolution was correlated with dissolved organic carbon ($R = 0.916$, $p < 0.0001$). Ligands >3 kDa, presumably fulvic acid from the SPEs, complexed Cu driving solubility; the addition of plant exudates further increased solubility 1.5–3.5×. The root-colonizing bacterium decreased dissolved Cu in sand pore waters from planted systems due to metabolism of root exudates. Batch solubility studies (10 mg L⁻¹ Cu) with the soil SPEs and defined solutions containing bicarbonate or fulvic acid confirmed elevated CuO nanoparticle solubility at >7.5 pH. Nanoparticle dissolution was suppressed in batch experiments compared to sand, via nanoparticle organic matter coating or homoconjugation of dissolved organic matter. Alterations of CuO nanoparticles by soil organic matter, plant exudates, and bacteria will affect dissolution and bioavailability of the CuO nanoparticles in alkaline soils.

Received 30th May 2020,
Accepted 3rd August 2020

DOI: 10.1039/d0en00574f

rsc.li/es-nano

Environmental significance

Dissolution of metal oxides in alkaline environments, such as calcareous soils, is sometimes incorrectly considered negligible due to the high pH. However dissolved organic carbon concentration, rather than pH, controlled the concentration of dissolved Cu from copper oxide nanoparticles in calcareous soil pore waters varying in organic matter concentration. Soil management, root exudates, and root-colonizing bacteria altered the dissolved organic carbon concentration. Thus, agricultural applications of copper oxide nanoparticles, and perhaps other metal oxides, may have higher dissolution in alkaline soils and the crop rhizosphere than would be expected based solely on pH.

Introduction

CuO nanoparticles (NPs) may be formulated into agricultural fertilizers and agents that improve plant stress tolerance.^{1–4} CuO NPs have complex interactions with soil microbes, soluble soil components, and plant roots,^{5–7} altering the fate

of NPs in the soil rooting zone. Recent reports indicate that the bioavailability of the dissolved Cu ion from CuO NPs, in particular, is closely associated with CuO NP toxicity.^{5–9} Qiu and Smolders observe no nanospecific toxicity of CuO NPs to barley in six soils ranging in pH from 5 to 7.⁹ Gao *et al.* find that soil ~pH 5.7 freshly spiked with CuO NPs is not toxic to wheat, although aging for 28 d causes toxicity; the difference is attributed to NP dissolution.⁷ Velicogna *et al.* see no difference between toxicity from CuO NPs or Cu salt, whether introduced to soil or soil with biosolids, to northern wheatgrass or red clover when the levels of resulting free Cu ions are considered.⁸ Pu *et al.* observe that CuO NP toxicity to maize in a pH 6.6 soil is controlled by bioavailable Cu released from the NPs.⁶ However, Shang *et al.* find that CuO

^a Utah Water Research Laboratory, Department of Civil and Environmental Engineering, Utah State University, Logan, UT 84321, USA.

E-mail: joshua.hortin@aggiemail.usu.edu, joan.mclean@usu.edu

^b Department of Biological Engineering, Utah State University, Logan, UT 84321, USA

^c Department of Plants, Soils, and Climate, Utah State University, Logan, UT 84321, USA

† Electronic supplementary information (ESI) available. See DOI: 10.1039/d0en00574f

NPs coated with maize root exudates are more toxic to maize in hydroponics, as measured by seedling growth rate, than uncoated NPs or an equivalent dose of Cu ions complexed with maize root exudates.¹⁰ The increased toxicity to maize of coated NPs is attributed to increased Cu in the root, possibly *via* reduced NP aggregation or enhanced Cu dissolution. Several organic and inorganic Cu complexes are bioavailable to wheat roots.^{5,11,12} Differences in bioavailable Cu complexed to root exudates or other organic material may help explain the apparently-conflicting maize results, and highlights the importance of understanding Cu dissolution and complexation in the presence of soil components.

While CuO is considered relatively insoluble in water, only low levels ($\mu\text{g L}^{-1}$) of free Cu ions are needed to provide significant toxicity to aquatic and plant life.¹² NP dissolution depends on physical properties of the NPs (such as size, aggregation, and morphology), characteristics of the solution (such as pH, ligand availability) and surface chemistry (such as capping agents or coatings).¹³ Dissolution of free Cu ions from mineral CuO is largely controlled by pH, with a theoretical increase of an order of magnitude per 0.5 unit pH decrease. Minimal Cu solubility is found at pH 9–11, although above pH 11, CuO solubility increases slightly due to complexing with hydroxide ions.¹⁴ Prior studies confirm increasing dissolution of CuO NPs with decreasing solution pH^{15,16} and through Cu ion complexation with organic ligands including many amino acids,^{15–17} low molecular weight organic acids (LMWOAs),¹⁸ metabolites in wheat root exudates,¹⁹ and the soil factors humic^{15,20} and fulvic acids²¹ (HA and FA, respectively). Dissolved natural organic matter (DNOM) in soils, including FA/HA, may also coat CuO NPs,^{15,20,22–24} reducing NP solubility in some,^{22,24} but not all studies (Table S1†).^{15,20} Inorganic anions, such as chloride²⁵ and carbonate,²⁶ could increase CuO NP solubility due to complex formation. Phosphate alters CuO NP surface chemistry,²² but the effect on solubility is unclear.

Cu, due to its high affinity for surface of soil minerals and organic matter even under acidic conditions, does not display a strong pH dependency controlling sorption²⁷ or plant uptake.^{28,29} Alkaline soils are frequently assumed to have low metal solubility and bioavailability due to pH,³⁰ but DNOM and aqueous carbonates could dissolve Cu *via* complexation at levels comparable to a low-pH soil. Therefore dissolution and bioavailability of CuO NPs at high pH cannot be neglected.

Dissolution is also influenced by the factors released from soil life forms, such as metabolites in root and bacterial exudates. Wheat root exudates contain amino acids, LMWOAs, and the iron siderophore, 2'-deoxymugineic acid (DMA); these compounds may enhance CuO NP dissolution and shoot uptake.^{5,19} Furthermore, the composition of the root exudates changes with increasing CuO NP dose.¹⁹ Bacterial secretions, such as the iron siderophore pyoverdine that also complex Cu, similarly increase solubility of CuO NPs.^{31–34} While the effects of individual bacteria,^{31,32} wheat,^{7,19} or soil^{35,36} on CuO NP dissolution have been

examined, there are little data on the effects of combinations of these environmental factors.

The size of the NPs present challenges when measuring NP solubility. The classic definition of water quality for dissolved metals, as those that pass through a 0.45-micron filter,³⁷ is not applicable for sub-100 nm sized metals. Thus, techniques for measuring CuO NP solubility must remove the suspended solid phase nano- and micro-particle fractions from the dissolved fraction. Specialized techniques, such as single particle inductively coupled plasma mass spectrometry (ICP-MS) or field flow fractionation ICP-MS are sometimes used but are not available to all analysts. Therefore, two widely available NP separation techniques (centrifugation and ultrafiltration with molecular weight cutoff of 3 kDa) are selected for this work. These techniques used in combination also yield information about the size distribution of Cu-DNOM complexes.

Characterizing added NPs in soil is, as of yet, extremely difficult, owing partially to the challenge of separating engineered NPs from bulk soil³⁸ and from natural NPs. Thus, a simplified soil and plant system, using sand as the growth matrix and augmentation with soil saturation paste extracts (SPEs), could be of use to identify factors that influence NP solubility⁵ leading to better understanding of how CuO NPs interact with microbes, soil components, and plants when used in agricultural settings. Many studies utilize hydroponics, but roots in hydroponic studies are different than those grown in soil, and results of toxicity studies derived from hydroponics often yield different toxicity constants than soil studies.³⁰ Plants grown in a sand matrix have similar root morphology to plants grown in soil, and there is better prediction of metal toxicity from sand culture than hydroponic culture.³⁰

The objectives of this study were to examine: 1) the solubility of CuO NPs, and the causal mechanisms involved, as affected by agricultural soil SPEs, wheat roots, and a root-colonizing bacterium, *Pseudomonas chlororaphis* O6 (PcO6);^{33,34} 2) the solubility of CuO NPs and the mechanisms involved in batch solubility studies with the SPEs compared with fulvic acid, phosphate, and bicarbonate; and 3) potential coatings on NPs after exposures to SPEs, and metabolites from PcO6 and/or wheat.

Materials and methods

Experimental design

CuO NP solubility in 3.34 mM $\text{Ca}(\text{NO}_3)_2$ and SPEs was determined in sand matrices and in batch solubility studies. The sand matrix experimental design, setup, and methods are described in detail in Hortin *et al.*⁵ This former work⁵ examined wheat responses to CuO NPs in a sand and SPE/ $\text{Ca}(\text{NO}_3)_2$ matrix, and thus only considered planted samples with and without CuO NPs. This paper extends the work to examine transformation of the CuO NPs in the SPE/ $\text{Ca}(\text{NO}_3)_2$ -amended sand matrix, with and without the growth of wheat and root colonization by PcO6. The combination of the two

NP conditions (with/without), two planted conditions (with/without), two bacterial conditions (with/without), and three SPEs and one 3.34 mM $\text{Ca}(\text{NO}_3)_2$ solution forms a $2 \times 2 \times 2 \times 4$ factorial design (Table S2†). Thus, the influence of the plant, bacterium, and differing SPEs on CuO NP transformations could be determined individually and in combination. The batch solubility studies confirmed observations made in the sand study and also yielded additional information about the kinetics of CuO NP dissolution in SPEs to supplement the sand-matrix experiments.

Soil saturation paste extracts and bacterium

Three soils were collected from agricultural sites in Cache County, UT, USA in late summer 2016 from depths of 0–10 cm. The three selected soils (Millville series, coarse-silty, carbonatic, mesic *Typic Haploxerolls*) had similar pH values between 7.7 and 7.8, but varied in crop management practices so that DNOM concentration differed. Soil characteristics, the cropping history and cultivation techniques are provided in Table S3.† SPEs were generated from these soils per standard methods with saturation pastes.³⁹ Characteristics of the SPEs after filter sterilization (pH, EC, soluble cations, anions, and organic matter) are given in Table S4.† *PcO6*, originally isolated from a field-grown wheat root, was used as a model root colonizing bacterium. *PcO6* preparation methods and usage conditions are described in Hortin *et al.*⁵

CuO NP wheat growth conditions

CuO NPs (Sigma-Aldrich) used in this study were thoroughly characterized.^{5,40} Briefly, the CuO NPs have a nominal size of 50 nm with 46 nm average diameter and 38 nm median diameter as measured by scanning electron microscopy, have an irregular rounded shape, are >99.3% pure as measured by metal digestion and analysis, were identified as crystalline tenorite by X-ray diffraction, have no surface alteration, and have negative zeta potentials in 1 mM KCl in the working pH range of 6.1–7.5. Preparation of white silica sand (UNIMIN Corp, ID), amendment with 100 mg kg^{-1} Cu as CuO NPs by 30 min high speed shaking as needed, and autoclave-sterilization of Magenta boxes (Sigma-Aldrich, V8505, $10 \times 7 \times 7$ cm) was performed as described in Hortin *et al.*⁵ The sand matrix was superior to hydroponics or whole soil matrices for testing the objectives (see Introduction). The NP dose was chosen because it is sublethal to wheat and *PcO6* colonizing its roots, but causes substantial root shortening.¹⁹ The autoclaving process is not expected to alter the fully-oxidized CuO NPs.¹⁹ A schematic of the preparation of materials preparation is found in Fig. S1.†

The factorial treatments were designed to give differing combinations of CuO NPs with wheat, *PcO6*, and the three SPEs or a 3.34 mM $\text{Ca}(\text{NO}_3)_2$ solution. The 3.34 mM $\text{Ca}(\text{NO}_3)_2$ solution has an ionic strength approximately in the middle of the values for the three SPEs and has no dissolved organic

matter. Each treatment had triplicate boxes and was repeated for a total $n = 6$. Each sand-filled box received either 45 mL of sterile 3.34 mM $\text{Ca}(\text{NO}_3)_2$ (termed the “electrolyte” treatment) or 0.2 micron-filter sterilized SPEs (named OrgM, AgrM, GarM) and was mixed under sterile conditions. The ratio of water to sand was 1.5 times field capacity.¹⁹ Inoculation with *PcO6* involved adding a suspension of 5.6×10^4 CFU per mL cells to the sterilized sand. Pre-germinated, surface-sterilized wheat seeds (Dolores variety, hard red winter wheat) were planted and grown for 10 days under 18 h photoperiod as previously described.⁵ A schematic of the planting procedures is found in Fig. S1.†

Extraction and analysis of pore water from the sand matrix

Planted and unplanted sand-filled Magenta boxes were harvested and analyzed at 10 d.⁵ A schematic of the harvesting procedures is found in Fig. S1† and additional methodology not previously used is described below. The term “sand pore water” (sand PW) indicates any solution withdrawn from the planted or unplanted sand after 10 days, whereas the term “SPE”, saturated paste extract, identifies the extracts from the three soils (one of the factors of this study).

The sand in each box was wetted with 45 mL of sterile deionized water and allowed to equilibrate for 15 minutes. Seedlings were gently removed from the sand, the roots and shoots were sectioned from just below and just above the coleoptile, and roots and shoot were dried. Cu in the roots, shoots, and sand samples was determined after hot nitric acid digestion^{41,42} by ICP-MS (Agilent 7700x, USEPA method 6020). Also, one root per planted box and one 15 μL aliquot of sand PW were placed on Luria-Bertani agar plates to verify the presence (or absence) of *PcO6* and/or contaminating bacteria; *PcO6* was always detected from inoculated boxes and was absent in non-inoculated treatments. Endophytic contamination of the wheat seed in planted samples was noted but these bacteria did not detectably affect the pore water chemistry.⁵

The sand PW was extracted by vacuum extraction of 300 g sand through a sterile glass funnel stoppered with glass wool. The pH and EC were measured in an aliquot of sand PW by standard methods³⁷ and free Cu^{2+} ions by ion selective electrode (Orion 96-29 Ionplus).⁴³ Other aliquots of sand PW (4.5 mL) were centrifuged (Eppendorf centrifuge 8504, Eppendorf rotor F45-30-11) at $20\,800 \times g$ for 15 minutes, a time and speed calculated by the Stokes–Einstein equation to pellet CuO NPs larger than 30 nm, and the supernatant was collected (3 mL). Additionally, 4 mL of uncentrifuged sand PW was filtered by a triple-pre-rinsed 3 kDa ultrafilter to partition dissolved Cu complexed to DNOM <3 kDa from dissolved Cu complexed to DNOM >3 kDa and NPs. The ultrafilters permitted a $93 \pm 2.3\%$ and $92 \pm 1.6\%$ (mean \pm standard deviation, $n = 3$) recovery of Cu ions in the filtrates when tested with 0.5 and 5 mg L^{-1} Cu^{2+} from $\text{Cu}(\text{NO}_3)_2$, respectively. The filters were used after triple rinsing per the

manufacturer's instructions⁴⁴ and released no glycerin, as measured as dissolved organic carbon (DOC). Previously, centrifugation was shown to remove CuO NPs >30 nm and ultrafiltration removed NPs >2 nm in wheat root exudates from a sand matrix.¹⁹

Dissolved metals in both the centrifuged and ultrafiltered portions were measured by ICP-MS, and DNOM was detected using a carbon analyzer (Apollo 9000, Teledyne Tekmar) by standard methods.³⁷ Hereafter, DOC is used in the discussion of the organic matter from SPEs, wheat and/or bacterial exudates. DOC is in units of mg L⁻¹ C and is not corrected for the other molecular components of DNOM.

NPs were not adequately removed by centrifugation, from visual inspection, from the sand PW obtained from unplanted sand with 3.34 mM Ca(NO₃)₂. To eliminate overestimation of dissolved Cu due to suspended NPs for this particular treatment, only the ultrafiltration results are reported, as noted in the text and figure captions. The unplanted electrolyte treatments are marked in the treatment schematic in the ESI† (Table S2). NPs were fully removed in other treatments, and a justification of this point is found in the ESI† (Fig. S2). It is proposed that the absence of DOC in the unplanted electrolyte treatments reduced agglomeration and a portion of the NPs remained suspended, limiting the effectiveness of centrifugation. DOC from the SPEs or root exudates, adsorbed to CuO NPs, lowers the isoelectric point of CuO NPs, creating opportunity for divalent cation-bridging induced flocculation enhancing separation with centrifugation. All treatments besides the unplanted electrolyte treatments contained DOC in the sand PWs.

XAFS analysis

To access the speciation of Cu in CuO NP samples, X-ray absorption fine edge spectroscopy (XAFS) was used. The samples were air-dried NP pellets collected by centrifugation of the sand PWs.¹⁰ The dried pellets were removed with a clean pipette tip and brushed onto layers of Kapton tape. Samples were analyzed on beamline 20-ID at the Advanced Photon Source of Argonne National Laboratory. XAFS regions were collected in fluorescence mode at six separate points per sample. Replicate samples were combined in layers to obtain a sample thick enough for XAFS spectroscopy. Dwell times were set at 20 minutes to avoid reduction of Cu(II) → Cu(I), which occurred for 1–2 hour dwell times during early data collection. No further sample reduction was observed over the course of the XAFS measurements. Reference standards included unaltered CuO NPs, cupric phosphate, Cu-FA, Cu-HA, cupric acetate, cupric carbonate, cupric sulfate, cupric sulfide, cuprous sulfide, and copper foil. XAFS data on the aqueous sand PWs (with and without CuO NPs removed) was also collected on select frozen (77 K) samples on beamline 20-BM at the Advanced Photon Source in fluorescence mode. Replicate scans were collected on each sample (4–10 scans depending on Cu concentration). Standards measured in the aqueous phase were complexes of

Cu with acetate, nitrate, citrate, cysteine, FA, HA, DMA, and gluconate.

Batch CuO NP dissolution studies

Batch CuO NP dissolution studies were performed in triplicate in 100 mL of SPE or 3.34 mM Ca(NO₃)₂ at a dose of 10 mg L⁻¹ Cu from CuO NPs contained in 250 mL glass Erlenmeyer flasks. A schematic of the batch dissolution treatment setups is shown in the ESI† (Fig. S3). The concentration of CuO NPs was chosen to saturate the SPEs with Cu, because geochemical models predicted the highest concentration of Cu in any SPE to be ~4 mg L⁻¹ Cu. All glassware was acid-rinsed with 50% nitric acid and DI water to eliminate metal contamination, and autoclaved prior to use. Ca(NO₃)₂ solutions were autoclaved and SPEs were filter-sterilized with a 0.2-micron filter. As the initial solution pH varied, pH was adjusted to a constant 7.5, to mimic the initial pH of the SPEs, using CO₂ gas or minimal NaHCO₃ solution prior to addition of NPs, after which no further pH control was used. Other pH modifiers and buffers were considered, including biologically compatible Good's buffers and inorganic buffers such as phosphate. Copper, however, complexes with some of Good's buffers⁴⁵ and precipitates with phosphate. The use of Good's buffers would also interfere with the DOC analysis.

The batch dissolution treatments were the three SPEs, a control solution of 3.34 mM Ca(NO₃)₂, and three 3.34 mM Ca(NO₃)₂ solutions with added defined components: alkalinity (as bicarbonate, 750 mg L⁻¹ CaCO₃ as NaHCO₃), FA (20 mg L⁻¹ C as Suwannee River FA), or phosphate (5 mg L⁻¹ PO₄-P). Follow-up batch dissolution experiments of CuO NPs were also performed on dilutions of the three SPEs with equal ionic strength Ca(NO₃)₂ (80% SPE, 60% SPE, 40% SPE, 20% SPE, and 0% SPE) to test the influence of varying organic matter concentrations on NP solubility. All treatments were shaken on a rotary shaker at 200 RPM, in a constant-temperature room at 25 ± 1 °C in the dark for up to 240 h. Well-mixed samples (7 mL) were taken with sterile pipettes without replacement at 0, 2, 4, 8, 24, 48, 96, 144, and 240 h and pH, EC, and dissolved Cu were measured. Follow-up experiments were only sampled at 48 h.

Dissolved Cu was measured at all time points by ICP-MS after centrifugation and ultrafiltration, as previously employed. Unlike the sand PWs, centrifugation effectively removed all NPs due to the lower NP dose, even in the electrolyte treatment without DOC; there was no significant difference in dissolved Cu between centrifuged or ultrafiltered samples for the batch electrolyte treatment (Fig. S2†). Samples of particulates from the suspensions were isolated by centrifugation, the supernatant was carefully removed with a pipette,¹⁰ and the pellet was stored under desiccated air for several days until analysis by Fourier transform infrared spectroscopy (FTIR) with attenuated total reflectance (Nicolet 6700) to determine NP coatings. The pellets were resuspended in 5 µL DI water¹⁰ and dried on a

glass slide before transferring the sample to the FTIR crystal. Triplicate FTIR data were collected in attenuated total reflectance mode over 250 scans from 525–4000 cm^{-1} .

Data analysis and statistics

To facilitate sample recovery, the sand-filled Magenta boxes were diluted with sterile water at harvest; dilution factors for the measured constituents were calculated as previously described to correct measured concentrations to original concentrations.⁵ Dissolved copper and DOC were analyzed in samples with CuO NPs by three way ANOVA (factors: SPE or electrolyte, presence/absence of wheat, and presence/absence of *PcO6*) in JMP 8 (ref. 46) followed by the Tukey honestly significant difference (Tukey HSD) test. In samples lacking CuO NPs, dissolved Cu was not present above the SPE background and thus was not included in the three way ANOVA. A log or square root transformation was used where noted to maintain normal distribution of the residuals. Pearson's correlations were used to ascertain the significance and strength of the relationships between dissolved Cu and other measurements.

XAFS spectra of CuO NP and dissolved Cu samples were analyzed with Athena (Demeter 0.9.25).⁴⁷ Linear combination fits were applied to the XAFS spectra using Athena. Standards were selected by testing fits of all combinations of all standards using the combinatorics feature in Athena, and the lowest *R*-factors were consistently found with combinations of CuO NPs, Cu-acetate, and Cu-sulfate; these standards were further confirmed by principal components analysis in Athena. Samples were considered significantly different from each other if the component fits and their standard deviations (as described by Ravel⁴⁸) did not overlap.

Batch dissolution data were fitted by *R* (ref. 49) to the first order kinetic equation:

$$C_{\text{Cu}} = C_{\text{Cu},0} \times e^{-k \times t} + C_{\text{Cu},\text{eq.}} \times (1 - e^{-k \times t}) \quad (1)$$

where C_{Cu} represents the concentration of dissolved Cu at any time *t* (hours), $C_{\text{Cu},\text{eq.}}$ represents the estimated dissolved Cu equilibrium concentration, $C_{\text{Cu},0}$ represents the initial measured dissolved Cu, and *k* represents the rate (in h^{-1}). Model quality was evaluated by residual distribution and root mean squared errors (RMSE).

A geochemical equilibrium model (MINTEQA v 3.1)⁵⁰ was used to compare theoretical dissolved Cu to actual measurements. The conditions of the model were the composition of the sand PWs at harvest, including input of FA and HA (if present) through the NICA-Donnan model using default FA/HA parameters, a crystalline CuO tenorite solid phase, closed atmosphere to allow alkalinity input, and no precipitation allowed. Selected metal–DMA and metal–gluconate stability complexes were added to the database from literature after correction to *I* = 0 by the Davies equation (Table S5†).¹⁹ There are currently no NP-specific solubility constants for tenorite, but CuO NPs >20 nm are not expected

to have significantly more solubility than “bulk” sized particles.⁵¹

Results and discussion

NPs primarily remained in the solid phase in sand matrices

After 10 d wheat seedling growth with 100 mg Cu per kg sand from CuO NPs, the distribution of Cu in the sand (undissolved), plant (roots and shoot), and dissolved in sand PWs in planted systems with and without bacteria was $85.5 \pm 12.3\%$, $1.2 \pm 1.2\%$, and $0.58 \pm 0.29\%$ (mean \pm SD), respectively. The total mass balance was $88.6 \pm 12.6\%$. In unplanted systems with and without bacteria, $88.2 \pm 10.8\%$ Cu from the NPs remaining in the sand and $0.22 \pm 0.19\%$ was dissolved in sand PWs; the total mass balance was $89.7 \pm 10.8\%$. The sand Cu and overall mass balance were not significantly changed by the presence of wheat, SPEs, root colonization by *PcO6*, or any combination of factors (data not shown). The maximum percentages of Cu in the plant and dissolved aqueous phase in any treatment were 2.0% and 1.1%, respectively. Extraction of the sand PWs showed some CuO NPs to remain in suspension before centrifugation or ultrafiltration; black-colored suspensions with visible particle agglomerates were observed in the initial extracts (Fig. S4†). The mass of suspended CuO NPs was not measured in this study, but this material could account for the 10–11% that was missing from the mass balance analyses.

These results suggest that CuO NPs, at high doses in a solid matrix, could persist for long periods of time, dissolving as ligands become available and/or as pH allows. If a soil phase is continuously flushed by irrigation or rainwater and the aqueous phase remains undersaturated with respect to Cu^{2+} , the dissolution of CuO NPs would continue indefinitely, as noted by Kent and Vikesland.⁵²

Dissolved copper was dependent on dissolved organic matter

Dissolved Cu, defined as ionic or complexed, was measured after removal of NPs by centrifugation in each of the treatments. As described in the Materials and Methods section, due to inadequate removal of NPs with centrifugation for the unplanted electrolyte sand PW, the results for this treatment were from ultrafiltration rather than centrifugation.

A three-way ANOVA showed the interaction of SPE or electrolyte, wheat, and *PcO6* were factors with significant impact on dissolved Cu (Fig. 1A). The same three-way interaction was also significant for DOC (Fig. 1B) and pH (Fig. 1C). The correlation between dissolved Cu and DOC in all samples with CuO NPs was $R = 0.916$ ($p < 0.0001$), the highest correlation of dissolved Cu to any other variable observed in this study (Table S6, Fig. S5†). The correlation of pH and dissolved Cu was also significant ($R = 0.292$, $p = 0.004$), but dissolved Cu and pH increased together, contrary to predicted thermodynamics. This finding shows that the influence of DOC overrode the influence of pH on CuO NP dissolution. While pH was influenced by wheat and bacteria

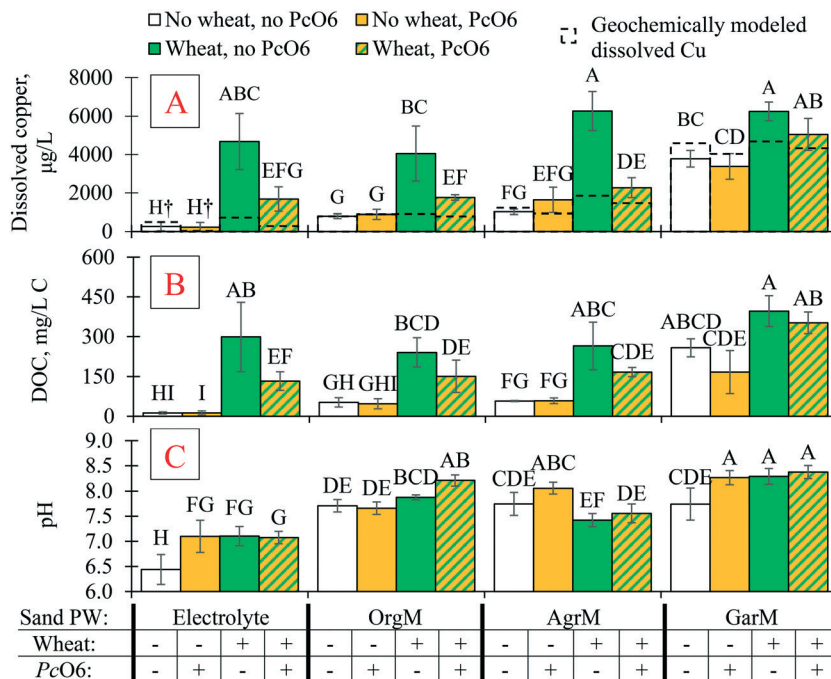


Fig. 1 The three-way interaction of wheat, PcO6, and SPE or electrolyte on sand PWs for: (A) dissolved Cu after centrifugation, (B) DOC, and (C) pH. Amendments to the sand were 3.34 mM $\text{Ca}(\text{NO}_3)_2$ (electrolyte) or SPEs from three alkaline soils, OrgM, AgrM, or GarM. The presence (+) and absence (-) of wheat and PcO6 is shown in the table below the charts. The dashed bars overlaying graph a show the geochemical model predicted concentration for dissolved Cu. Bars are average of 6 replicates. Error bars represent the 95% confidence interval and do not determine significance but are given to show the general spread of the data. Bars with differing letters are statistically different after Tukey HSD test. A square root transformation was required to maintain normal distribution of the residuals for dissolved Cu. † values for this treatment were from ultrafiltered samples, i.e. $\text{Cu} < 3$ kDa, as explained in Materials and methods section.

(Fig. 1C), pH had no significant influence in determining dissolved Cu. The finding that DOC was highly correlated with dissolved Cu in this study agrees with Gao *et al.*,³⁵ though the influence of pH on dissolution kinetics was not tested in this design. Gao *et al.*³⁵ found that soil organic matter predicted the steady-state solubility of CuO NPs in soil, and that pH predicted the dissolution kinetic rate.

The growth of wheat increased dissolved Cu and DOC in every sand PW over the levels detected from nonplanted systems (green bars compared to white bars, Fig. 1A and B) except for DOC in the treatment with GarM SPE. Release of plant metabolites as root exudates is proposed to account for the increase in DOC. By inference the released metabolites enhanced dissolution of the CuO NPs. In the planted systems, the presence of the root-colonizer PcO6 decreased dissolved Cu compared to non-inoculated plants (green/orange striped bars compared to green bars) except with the GarM treatment. However, PcO6 only decreased DOC from the plants grown in the electrolyte treatment. The DOC in the electrolyte treatment was all plant-derived, whereas the SPEs contained non-degradable humic material. Thus, PcO6 selectively metabolized root exudates, such as LMWOAs and amino acids that function as Cu chelators.⁵ Pseudomonad cells, such as those on the root surface, also sorb Cu,⁵³ which could explain a reduction in dissolved Cu without a reduction in DOC. The presence of the bacterium alone in nonplanted sand (white vs. orange bars, Fig. 1A) had no effect on NP

dissolution, though bacterial metabolism was probably limited from lack of available nutrients. The readily metabolizable compounds from root exudation were already absent from the SPEs that were used in the studies (Table S4†).

Additionally, differences among the SPE or electrolyte treatments were seen. The sand PWs from the electrolyte, OrgM (42.7 mg C per L), and AgrM (73.4 mg C per L) treatments, which contained no or lower DOC initially, had similar patterns in DOC exudation and Cu dissolution; in these treatments, the plants generated significant increases of DOC and significant increases in dissolved Cu. In the GarM treatment which had high initial DOC (305 mg C per L), plants did not generate significant additional DOC, even though dissolved Cu increased. Despite the wide range of initial DOC values of the treatments, DOC and dissolved Cu at harvest were approximately equal across all treatments. The GarM SPE also had higher salt and ionic strength contents relative to the other SPEs and electrolyte. Chloride particularly can reduce plant malate production (as seen for *Vicia faba*).⁵⁴ These results may imply that with planting, soils with high organic or salt contents will not dissolve significantly more Cu because the plants reduce or adjust their exudation.

The dissolved Cu values determined by geochemical modeling (dash lined bars, Fig. 1A) mostly agreed within the 95% confidence interval for analysis of sand PWs from the

systems without plants but showed more disparity for the sand PWs from planted samples. This difference could be due to incomplete characterization of active rhizosphere components or variability in plant exudation. However, these results demonstrated that both the increases in DOC from metabolites from the plant roots and compounds present in the SPEs increased CuO NP dissolution. Rhizosphere bacteria, such as *PcO6*, moderated root exudate composition, which in turn altered NP dissolution; likely, such interactions would also occur in native planted soils.

Wheat root exudates drove CuO NP dissolution

The size distribution of dissolved Cu from the sand PWs of the planted and unplanted sand matrices was determined by centrifugation and ultrafiltration with a 3 kDa filter. Concentration was assessed by ICP-MS and with a Cu ion-selective electrode. Four categories were defined: Total dissolved Cu (measured directly after centrifugation, NPs >30 nm removed), complexed Cu >3 kDa (calculated by centrifuged Cu – ultrafiltered Cu), complexed Cu <3 kDa (calculated by ultrafiltered Cu – free Cu), and free Cu (measured directly by ion-selective electrode). This procedure gives information about whether dissolved Cu was complexed to large molecules (>3 kDa, primarily FA/HA), small molecules (<3 kDa, primarily simple root metabolites), or was uncomplexed. Fig. 2 illustrates that the distribution of sizes for the dissolved Cu changed based on the presence of wheat. *PcO6* influenced free Cu ions but not Cu size distribution, so data with and without *PcO6* were pooled in Fig. 2. The fact that *PcO6* did not influence Cu size distribution indicates that the metabolism of plant-generated organic acids and production of bacterial metabolites did not alter the complexation size patterns of the dissolved Cu.

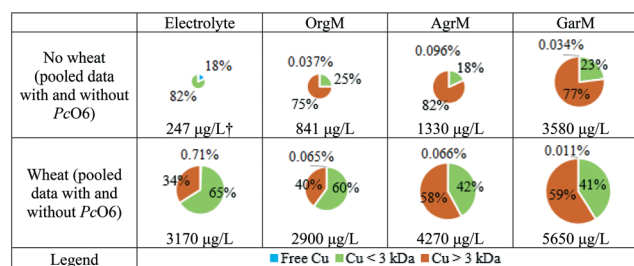


Fig. 2 Variations in the dissolved Cu size distribution in the sand PWs with treatments of electrolyte versus SPEs, with and without wheat growth, with CuO NPs. Data are pooled from systems with and without *PcO6* inoculation. Pie areas and text below pie charts represent total dissolved Cu and are average of 12 independent sample measurements. Text overlays are shown as the amount of total dissolved Cu (µg L⁻¹), and % of the total per size category. Overlays that do not add to exactly 100% are due to rounding effects after two significant figures. The 'no wheat' treatments were statistically different from the 'wheat' treatments in each SPE. † values for this treatment were from ultrafiltered samples, i.e. Cu <3 kDa, as explained in Material and methods section.

In the sand PWs obtained in non-planted systems, dissolved Cu was primarily (75–82%) in the >3 kDa range when the SPEs, OrgM, AgrM, and GarM were present. This size range is attributed to complexation with FA/HA present in the SPE to produce complexes >3 kDa. In the planted systems, there was increased total dissolved Cu (Fig. 1 and 2), and the proportion of Cu complexed to molecules <3 kDa was higher (41–60%, Fig. 2) in the SPEs due to complexation with low molecular weight metabolites in the root exudates. The highest percentage of dissolved Cu with <3 kDa size was in the planted electrolyte treatment, where only plant factors influenced the size of the Cu complexes, although some Cu >3 kDa was measured. While plants may produce some Cu-complexing molecules >3 kDa (as seen by Shang *et al.*¹⁰ for maize), such as proteins, sloughed root cap cells, or other components, most Cu-complexing molecules produced by wheat were <3 kDa. Similarly, maize root exudate metabolites <3 kDa were more effective at dissolving CuO NPs than root exudate metabolites >3 kDa.¹⁰ These results support that organic exudates from the roots are the driver behind the increase of soluble Cu <3 kDa in planted samples, while FA/HA derived from the soils are the major drivers of solubility for alkaline SPEs.

Free Cu²⁺ was a significant fraction of total dissolved Cu in the electrolyte solution with no plants (18%), but only 0.71% was measured in the planted sand PWs since dissolved Cu was complexed with root exudate metabolites. In the electrolyte solution from the unplanted sand, the ligands complexing Cu are unknown but could be hydroxide, carbonate, gluconate, or nitrate according to geochemical modeling.

Further speciation of the dissolved Cu in all treatments was attempted by linear combination fitting after XAFS, but failed because the dissolved Cu concentrations (<8 mg L⁻¹) were too low to be reliably measured and reconstructed through linear combination fits. However, the spectra collected, although noisy, confirmed that CuO NPs were absent after suspension in SPEs and centrifugation (Fig. S6†). Also, the dissolved Cu in the sand PWs from the different treatments was present only as oxidized Cu²⁺-complexes (Fig. S6†).

Free Cu ion levels were primarily controlled by SPE presence

There was no three-way interaction of wheat, SPE, and *PcO6* on free Cu ions in the sand PWs, but there were two significant two-way interactions: the interactions of SPE/wheat and SPE/*PcO6* (Fig. 3). Free Cu²⁺ ions were highest in the electrolyte sand PW, with or without wheat (Fig. 3), and these extracts had the lowest pH (Fig. 1C). There was also no HA/FA in the electrolyte sand PWs. Wheat growth did not change free Cu²⁺ in any sand PW. The presence of *PcO6* only reduced free Cu²⁺ levels in the electrolyte, probably by pH effects or ion sorption.⁵³ These results indicated that the SPE type was the most consequential in determining the availability of the free Cu²⁺ ion.

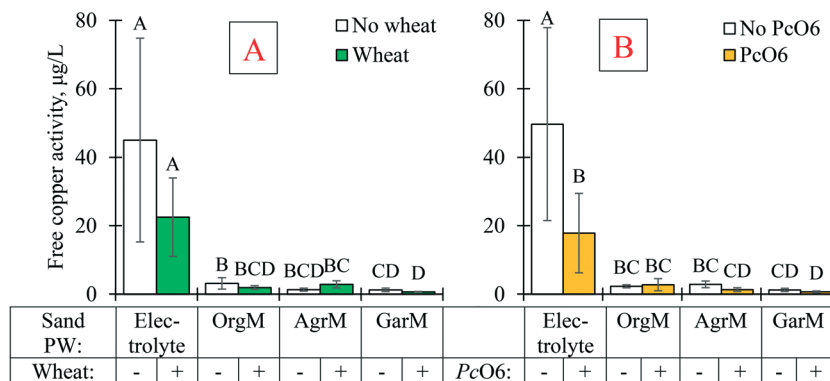


Fig. 3 The two-way interactions of wheat and SPE or electrolyte (A) and PcO6 and SPE or electrolyte (B) on free Cu^{2+} in the sand PW samples with CuO NPs. Amendment to the sand is 3.34 mM $\text{Ca}(\text{NO}_3)_2$ (electrolyte) or SPEs, OrgM, AgrM and GarM. The presence (+) and absence (-) of wheat or PcO6 is shown in the table below the charts. As a two-way interaction, PcO6 and non-PcO6 samples are pooled in graph A, and planted and unplanted samples are pooled in graph B; thus bars represent the average of 12 replicates. Error bars represent the 95% confidence interval and do not determine significance but are given to show the general spread of the data. Bars with differing letters are statistically different after Tukey HSD test. A logarithmic transformation was required to maintain normal distribution of the residuals.

Batch CuO NP dissolution studies

Batch dissolution studies were conducted to provide information about the relative importance of SPE components on NP dissolution, as well as a view of the effect of time on Cu dissolution. The tested soil PW individual components were alkalinity as bicarbonate, FA, and phosphate, which were present at different levels in the SPEs (Table S4†).

Over 10 days, most treatments reached a steady-state condition for dissolved Cu as defined by at least the final three dissolution values being statistically the same. Steady-state dissolution was reached immediately (0 h) with the electrolyte, at 8 h for FA, 24 hours for the alkalinity and AgrM PW treatments, and 48 h for the OrgM PW treatment. No steady state was reached in the GarM PW or phosphate treatment (Fig. 4). The pH also increased from 7.5 to range between 8.3–8.8 in all treatments by 240 h except with the

electrolyte treatment; steady state pH was reached at 0 h in the electrolyte, 4 h for AgrM PW, 8 h for OrgM PW and GarM PW, 24 h for FA and phosphate, and 48 h for alkalinity (Fig. S7†). Although a more alkaline pH thermodynamically inhibits Cu^{2+} solubility, there was no significant relationship between pH and dissolved Cu for all the treatments ($p = 0.1126$) at 240 h. These results again demonstrate the importance of DOC in governing CuO NP dissolution, particularly at high pH. Overall, FA was a more effective ligand than bicarbonate, and phosphate did not promote NP dissolution, as either a ligand or modifier of NP surface chemistry.

First order kinetic dissolution models described the formation of dissolved Cu in most treatments (Fig. 4, Table 1). Model residuals are shown in the ESI† (Fig. S8 and S9). Dissolved Cu was at steady state at 0 h in the electrolyte solution, so no kinetic model could be calculated. Dissolution in GarM SPE or phosphate did not reach steady state, indicating that kinetics may have followed a different order model. Consequently, the first order rate constants for GarM SPE and phosphate treatment, while still shown, were considered unreliable.

The rates observed in this study were within a large range, spanning three orders of magnitude, of those reported in other studies. The half-lives reported in this study, ranging from 7.8–31.1 h, were comparable to measurements by Vencalek *et al.*⁵⁵ of 30–32 h for CuO NPs in stagnant/stirred DI water (pH 5.8) and 29–73 h for stagnant/stirred freshwater mesocosms (pH 7.7, DOC 8.8 mg L^{-1}). The range of first order rate constants reported in Gao *et al.*³⁶ for a soil (pH 5.6), 4.58 and $5.42 \times 10^{-3} \text{ h}^{-1}$ for two NP doses, and the range reported in Jiang *et al.*²¹ for water (pH 6.3–7.0) with one of three sources of DOC, 2.02 – $9.36 \times 10^{-3} \text{ mol Cu per mol CuO per h}$, are lower by an order of magnitude than the measurements here. On the other hand, the range reported in Miao *et al.*³² for 10 mM NaCl with alginate, bovine serum albumin, or bacterial extracellular polymeric substances, 2.9–

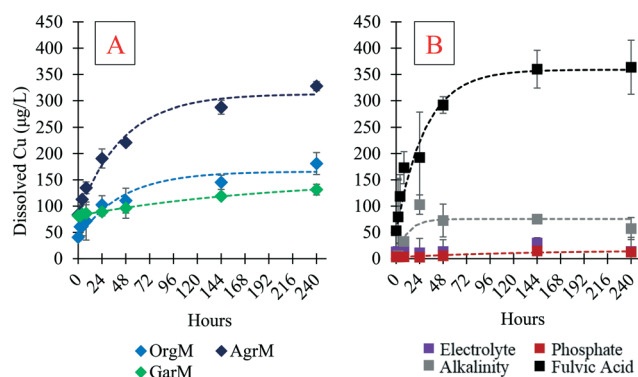


Fig. 4 Measured dissolved Cu and calculated first order kinetic models of dissolved Cu in all SPEs (A) and electrolyte, alkalinity (bicarbonate), phosphate, and fulvic acid treatments (B) as a function of time. Points are average of independent sample measurements ($n = 3$, except $n = 6$ in electrolyte and $n = 2$ in AgrM after 8 hours due to bacterial contamination of one sample). The dashed lines are the first order model results.

Table 1 First order model parameters of fits to measured dissolved Cu in all treatments (eqn (1)) and MINTEQ predicted Cu solubility. $C_{Cu,0}$ = initial dissolved Cu; $C_{Cu,eq}$ = dissolved Cu at equilibrium; k = first order rate constant; RMSE = root mean squared error of the model; $t_{1/2}$ = half-life of reaction

Treatment	MINTEQ model solubility ($\mu\text{g L}^{-1}$)	$C_{Cu,0}$ ($\mu\text{g L}^{-1}$)	$C_{Cu,eq}$ ($\mu\text{g L}^{-1}$)	$k \pm 95\%$ confidence interval (h^{-1})	RMSE ($\mu\text{g L}^{-1}$)	$t_{1/2}$ (h)
Electrolyte ^b	6.74	17.8	N/A	N/A ^b	N/A	N/A ^b
OrgM PW	571	40.7	166	$2.23 \times 10^{-2} \pm 1.16 \times 10^{-2}$	21.7	31.1
AgrM PW	819	83.6	313	$2.24 \times 10^{-2} \pm 0.74 \times 10^{-2}$	20.4	30.9
GarM PW ^a	3680	81.8	153	$5.04 \times 10^{-3} \pm 8.26 \times 10^{-3a}$	10.2	138 ^a
Alkalinity	27.3	3.1	75.6	$8.83 \times 10^{-2} \pm 7.17 \times 10^{-2}$	21.7	7.8
Fulvic acid	402	53.3	359	$3.39 \times 10^{-2} \pm 1.49 \times 10^{-2}$	48.8	20.4
Phosphate ^a	6.18	2.7	16.2	$7.50 \times 10^{-3} \pm 9.60 \times 10^{-3a}$	2.5	92.4 ^a

^a Indicates that treatment did not reach steady state in 240 hours, and first order rate estimate is considered unreliable. ^b Indicates that treatment was always at steady state.

$6.4 \times 10^{-1} \text{ h}^{-1}$, was greater by an order of magnitude than the measurements here. Kent and Vikesland⁵² reported that CuO NPs fully dissolved within hours in a flow-through system of DI water adjusted to pH 6.6 or 8.4; much faster rates than observed compared with closed systems. Gao *et al.*³⁵ found that the concentration of soil organic matter did not affect dissolution kinetics whereas pH did, so variability in rates is certainly influenced by soil/solution characteristics.

Unexpectedly, solubility of CuO NPs for a SPE in the sand (no plant or *PcO6*) was about an order of magnitude higher than the same SPE in a flask (for OrgM, $795 \mu\text{g L}^{-1}$ in sand vs. $181 \mu\text{g L}^{-1}$ in the flask; for AgrM, $1020 \mu\text{g L}^{-1}$ in sand vs. $328 \mu\text{g L}^{-1}$ in the flask; for GarM, $3780 \mu\text{g L}^{-1}$ in sand vs. $131 \mu\text{g L}^{-1}$ in the flask; data were from Fig. 1A compared to Fig. 4A endpoints). While dissolved Cu predicted using MINTEQ mostly agreed with the measured dissolved Cu from the sand matrix for each SPE (Fig. 1A), the concentrations of dissolved Cu seen in the flask studies were lower than the model for each SPE (Table 1). The apparent suppression of solubility could be due to two mechanisms: 1) the association of DOC molecules with other DOC molecules, resulting in homoconjugation to limit interactions with the NPs,⁵⁶ and 2) NP coating by DOC that would limit dissociation of the NPs.²² For instance, high concentrations of HA (20–100 mg L^{-1} HA) lower the $\log K^C$ of Cu–HA binding by 2.87–3.13;⁵⁶ FA is expected to behave similarly. NP coatings inhibited the solubility of CuO NPs in freshwater²² and stream water,²⁴ and release of Ag from Ag NPs in soil solutions.⁵⁷

The suspensions in both the sand and flasks were oversaturated with respect to the solid cupric phase, but the amount of surface area available for coating by DOC differed between the two systems. Each magenta box contained 300 g sand, 36 mg CuO NP (30 mg Cu), and 45 mL solution; whereas, each flask contained 1.2 mg CuO NP (1 mg Cu) and 100 mL solution. The sand and CuO NPs are estimated to have $0.1 \text{ m}^2 \text{ g}^{-1}$ and $29 \text{ m}^2 \text{ g}^{-1}$ (Sigma-Aldrich) of surface area, respectively, for a total surface area from the sand and NPs of 30.9 m^2 . The flasks contained about 0.029 m^2 , three orders of magnitude lower. Increased surface area in the sand box would provide more area for the DOC to coat, reducing coatings on the NPs and also lowering the effects of homoconjugation.

Three additional experiments were conducted to test the hypothesis that DOC limited solubility *via* NP coating in the batch solubility flask studies. In the first two experiments, the doses of CuO NPs in a sand magenta box and a flask with SPE were adjusted to have the same NP:solution ratio. When the CuO NP dose in a flask with SPE was set at 667 mg L^{-1} Cu (23.2 m^2 surface area) equivalent to a 100 mg kg^{-1} Cu per sand magenta box with the SPE (30.9 m^2 surface area), soluble Cu was the same between the two systems (Fig. S10†). In the second experiment, when the CuO NP dose in a sand-filled magenta box with SPE was set at 1.5 mg kg^{-1} Cu per sand (30.1 m^2 surface area) equivalent to the 10 mg L^{-1} Cu dose in the flask with SPE (0.029 m^2 surface area), soluble Cu was suppressed in the flask compared to the sand (Fig. S10†). This result shows that the suppression of NP dissolution occurred when the surface area was low in the flasks, with DOC coating more of the NPs or homoconjugation more active, limiting solubility.

In the third experiment, NP dose and surface area in a flask were held constant (10 mg L^{-1} Cu, 0.029 m^2) while SPEs were diluted in steps of 20% with an equal ionic strength $\text{Ca}(\text{NO}_3)_2$ solution, creating a range of DOC concentrations from 8.5 to 305 mg L^{-1} C across the three SPEs. The $\text{Ca}(\text{NO}_3)_2$ solution was used as a control with 0 mg L^{-1} DOC. All solutions were shaken for 48 h. Solubility in the OrgM and AgrM SPEs deviated from predicted values of the geochemical model (filled circles) at higher DOC levels but met predictions at lower DOC levels (Fig. 5). In the GarM SPE, the highest dissolution was measured at the lowest DOC concentration (Fig. 5). Further dilution of the GarM SPE would likely result in dissolution results approaching model predictions. The possibility of dissolved ions sorbing to the glass walls or to large colloidal organic matter, and thus not being measured as soluble Cu, was ruled out by no observable loss of added Cu ions in the SPEs over 48 hours (Table S7†). These findings demonstrated that at 10 mg L^{-1} Cu from CuO NPs and 0.029 m^2 surface area, coupled with DOC above $\sim 30 \text{ mg L}^{-1}$ DOC, restricted the solubility of CuO NPs.

Nanoparticle coating

In an attempt to shed more light on the potential NP coating by DNOM, the CuO NPs isolated after exposure to SPEs for 10

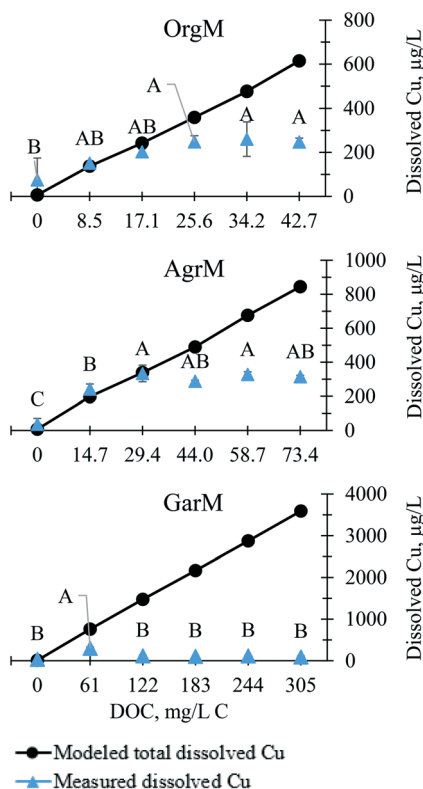


Fig. 5 Dissolved Cu concentrations from batch dissolution studies at 48 h measured after centrifugation (blue triangles) as a function of dilution of three SPEs at constant ionic strength. Measurements were compared to MINTEQA modeled Cu concentrations using default fulvic/humic acid complexation values in the NICA-Donnan model (filled black circles). Data points represent the average of three independent replicates, and error bars on measured dissolved Cu represent standard deviations. Measured Cu was analyzed by one-way ANOVA per SPE and differing letters indicate statistically different measurements.

d from the flasks were examined by FTIR. Also, NPs isolated from the sand matrix were examined by XAFS. Both techniques would reveal NP coatings,^{10,15,58} depending on the degree of coating and/or transformation.

Dissolved Cu is reported to have affinities, from greatest to smallest, for carboxyl (1250–1260 and 1720 cm^{-1}), polysaccharide (1038–1100 cm^{-1}), phenolic (1390–1400, 1280, and 1020 cm^{-1}), aromatic (1620, 850, and 780 cm^{-1}), amide (1660–1665 cm^{-1}), and aliphatic groups (2926, 2853–2856, 1440–1465, and 1350–1375 cm^{-1}).^{58–60} CuO NPs preferentially bind, in a similar order to dissolved Cu, from greatest to smallest, to carboxyl (1432 cm^{-1}), polysaccharide (1057 cm^{-1}), amide (1600 cm^{-1}), aromatic (842 cm^{-1}), and phenolic (913, 1300 cm^{-1}) groups.⁶¹ Covalent binding of Cu to functional groups quenches the FTIR signal of the group,^{58,59} but would allow the remaining functional groups in the structure, particularly weak-bonders like aliphatic groups, to be observed. Non-covalent bonds, such as adsorptive reactions, would also preserve the FTIR signal.

The FTIR spectra of CuO NPs from the SPEs were convoluted but showed clear changes in peaks in the organic fingerprint regions compared to the spectra of NPs exposed

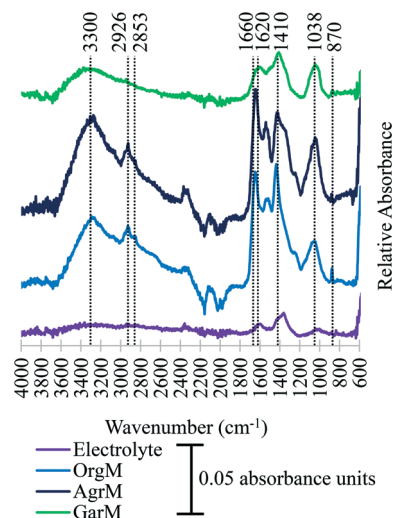


Fig. 6 FTIR scans of CuO NPs isolated from suspension in SPEs compared to CuO NPs isolated from suspensions in 3.34 mM $\text{Ca}(\text{NO}_3)_2$ (electrolyte). Dashed lines indicate important wavelengths for different groups with the potential to bind Cu: at 3300 (hydroxyl), 2926/2853 (aliphatic), 1660 (amide), 1620 (aromatic), 1038 (polysaccharide), and 1410/870 (carbonate) cm^{-1} .

only to electrolyte (Fig. 6). The spectra from all the SPEs samples had intensities above the corresponding signals from CuO NPs suspended in electrolyte to varying degrees for the aliphatic methyl and methylene (2926, 2853), hydroxyl (3000–3500), polysaccharide (1038–1100), and amide (1600–1665) groups. Shang *et al.*¹⁰ saw similar signal enhancements with CuO NPs coated with maize root exudates; there were increases at 1000–1150 cm^{-1} (alcohol, ether, and carbohydrate), 1600–1650 cm^{-1} ($\text{C}=\text{O}$), and 2500–3600 cm^{-1} (alcohols, phenols, carboxylates, amides). Carboxylic signals were not observed in the samples with any SPE treatment although they were expected from the FA content. This finding could be explained by the NPs or ions binding at the carboxylic acid groups to eliminate their signal. Characteristic inorganic carbonate peaks (~ 860 – 880 , ~ 1410 cm^{-1}) were apparent at relatively low levels in the NP samples. The varied FTIR fingerprints between the SPEs also suggested that the different dissolved organic materials in the pore waters from these alkaline soils lead to different types of coating on the NPs. The complexity of the existence of many functional groups, owing to the diverse types of DOC, made further interpretation of the spectra difficult and deserving of further research. The phosphate, alkalinity, and FA treatments were not examined by FTIR.

The XAFS spectra of all NPs incubated in the sand matrices appeared similar to each other and to the CuO NP standard, indicating that there was little change due to a specific treatment (Fig. 7). In the CuO NP standard (Fig. 7), the shoulder in the rising edge is attributed to the $1s \rightarrow 4p_\pi$ shake-down transition (an electron transfer from O to Cu), and the white line peak (maxima) is attributed to the $1s \rightarrow 4p_\sigma$ transition.⁶² In the spectra of the CuO NPs from the sand matrixes, the $1s \rightarrow 4p_\pi$ transition was suppressed and the

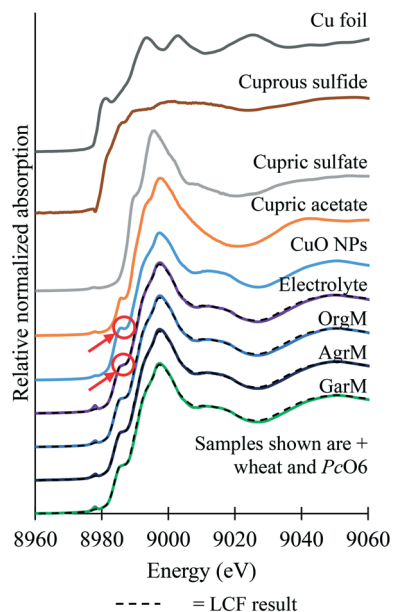


Fig. 7 Normalized X-ray absorption spectra of five standards (cupric sulfate, cupric acetate, CuO NPs, cuprous sulfide, and Cu foil) and CuO NPs from four sand PWs with wheat and PcO6. The red circles highlight subtle difference in the shoulder between environmentally exposed and pristine CuO NPs. The linear combination fitting (LCF) results are shown with dashed lines overlaying the sample spectra. The peak appearing just before 8980 is a monochromator glitch and present in all measurements, but preserved in this figure to restrict manipulation of the data.

white line $1s \rightarrow 4p_{\sigma}$ transition was increased relative to the standard (Fig. 7, annotations, Fig. S11†). There was no edge shift, indicating no changes in the oxidation state in any treatment.

To elucidate the composition of the samples, several standards were measured and linear combination fitting (LCF) was used. Combinations of the signals from cupric sulfate, cupric acetate, and CuO NPs consistently gave the best fit (lowest R -factor) to the NP samples, regardless of treatment. Cupric acetate was used to model Cu–carboxylic acid bonding, a preferred ligand for free Cu. In general, regardless of SPE or electrolyte, wheat growth or presence of PcO6, 80–90% of the Cu remained as CuO NPs, 10–15% as Cu-acetate, and 0–5% as Cu-sulfate (Table S8†). Results were similar whether the LCFs were applied to the normalized spectra, first derivative spectra, or $\chi(k)$ space; however, the first derivative and $\chi(k)$ trended towards greater amounts of CuO in the samples (85–95%) and less cupric acetate/sulfate (Tables S9 and S10†). The large differences in solubility of the CuO NPs in the different treatments, compared to the relatively minor differences in NP surface transformation, indicates that NP surface transformation was not a prerequisite or hindrance of dissolution in the sand matrices. If NPs from the batch dissolution studies had been measured by XAFS, there may have been a larger transformation of the NPs correlating with increased surface coating and the suppressed dissolution seen in those systems.

Peng *et al.*¹⁵ reacted CuO NPs with aqueous citric acid and HA for 48 h, and observed by XANES analysis a 5–13% transformation of the CuO NPs to an organic phase. Sekine *et al.*⁶³ incubated the same dose of CuO NPs as this study ($100 \text{ mg kg}^{-1} \text{ Cu}$) in two alkaline soils (pH 8.0) for five days and observed by XANES that 54–73% of the Cu transformed to Cu associated primarily with ferric oxyhydroxides and partially with DOC. Soils with higher pH reacted slower and had more Cu associated with the iron oxyhydroxides.⁶³ Gao *et al.*³⁶ also applied the same dose of CuO NPs as this study to a low-pH soil (pH 5.6) and found that 41–44% of the CuO NPs transformed to Cu–humic acid over 7–19 days, although the authors note that clay or metal oxide solid surfaces could contribute to the Cu–humic acid signal *via* the shared Cu–O bond of both surfaces. The large NP transformations observed by the soil studies, which were not observed in this study or that of Peng *et al.*¹⁵ were probably due to the lack of iron oxyhydroxides and other soil minerals in the aqueous solutions or the quartz sand used as the growth matrix. Soil minerals would provide a substantial surface area for sorption of Cu ions, which would drive the CuO NP dissolution reaction forward with the removal of Cu ions from solution. For example, the pH 5.6 soil sorbed 100% of the $100 \text{ mg kg}^{-1} \text{ Cu}$ dose when added as $\text{Cu}(\text{NO}_3)_2$.³⁶ Nevertheless, all the cited studies and this work indicated a portion of the CuO NPs were transformed to give signals characteristic of Cu-bound to organic ligands. The mineral phases of soil will have additional impact on the transformations, and probably bioavailability of CuO NPs in soils.

Conclusions

CuO NPs dissolution occurred at varied levels in all systems: \pm wheat, \pm PcO6, and regardless of whether sand was amended with SPEs or $\text{Ca}(\text{NO}_3)_2$ electrolyte. Wheat growth promoted Cu dissolution to values of $1\text{--}6 \text{ mg L}^{-1}$ in pore water. Colonization of the root with the pseudomonad decreased the dissolved and free Cu through mechanisms involving the catabolism of chelates in the root exudates, altered pH, and possibly sorption of ions to the microbial cell surface. The DOC in the sand PWs and the dissolved Cu were strongly correlated, with Cu complexation to components both below and above 3 kDa, indicating influence of both root exudates and larger HA and FA interactions. Free ionic Cu was low ($<25 \text{ } \mu\text{g L}^{-1}$) when SPEs and root exudates were present. These results indicate that CuO NPs dissolve in alkaline and calcareous soils dependent on the organic matter content. In alkaline conditions, plant toxicity of CuO NPs is unlikely to be derived through the influence of the free ion alone, but also from complexes. As such, plants will likely increase CuO NP dissolution, particularly in the rhizosphere of low organic matter soils due to enhanced production of exudates as observed for the SPE treatments from ArgM and OrgM compared to GarM soils, amplifying the bioavailability of Cu. At conditions and the dose of CuO NPs utilized in this study

(100 mg kg⁻¹ Cu), generally less than 1% of the NPs dissolved and, thus, the majority of the Cu remained in the solid, NP form, indicating that CuO NPs would persist in the alkaline/calcareous soil environment for long periods of time.

Batch dissolution studies confirmed the importance of FA as the main Cu chelator in SPEs. Bicarbonate ions also increased CuO NP dissolution. Dissolution could be suppressed by high concentrations of dissolved organic matter and low surface area availability. These results demonstrated mechanisms by which CuO NPs dissolve in soil. The suppressing effect of NP coating on CuO NP dissolution is probably limited in soil owing to the vast surface area presented by the soil minerals, minimizing the DOC coating interaction with the NPs or homoconjugation. Overall, the combined effects of crops, plant-colonizing microbes and soil organic matter could have large effects on the dissolution of CuO NPs, and hence their bioavailability to agricultural crops – in some cases for beneficial effects, but in other cases for unexpected negative effects.

Conflicts of interest

There are no conflicts to declare.

Acknowledgements

We gratefully acknowledge funding provided by the Utah Water Research Laboratory under the State of Utah Mineral Lease Fund, National Science Foundation grant #1705874, and Utah Agricultural Experiment Station grant #UTA-01341. We thank Jessica Cooper for the use of her art in the TOC abstract, and Tessa Guy, Joe Stewart, Paul McManus, Jeremiah Lamb, Kaisa Patterson, Nicki Thornhill, and Rashelle Wegelin for laboratory assistance.

References

- W. H. Elmer and J. C. White, The use of metallic oxide nanoparticles to enhance growth of tomatoes and eggplants in disease infested soil or soilless medium, *Environ. Sci.: Nano*, 2016, **3**, 1072–1079.
- C. M. Monreal, M. DeRosa, S. C. Mallubhotla, P. S. Bindraban and C. Dimkpa, C., Nanotechnologies for increasing the crop use efficiency of fertilizer-micronutrients, *Biol. Fertil. Soils*, 2016, **52**, 423–437.
- C. O. Dimkpa and P. S. Bindraban, Nanofertilizers: New products for the industry?, *J. Agric. Food Chem.*, 2018, **66**, 6462–6473.
- C. O. Dimkpa, P. S. Bindraban, J. Fugice, S. Agyin-Birikorang, U. Singh and D. Hellums, Composite micronutrient nanoparticles and salts decrease drought stress in soybean, *Agron. Sustainable Dev.*, 2017, **37**, 1–21.
- J. M. Hortin, A. J. Anderson, D. W. Britt, A. R. Jacobson and J. E. McLean, Soil-derived fulvic acid and root exudates, modified by soil bacteria, alter CuO nanoparticle-induced root stunting of wheat via Cu complexation, *Environ. Sci.: Nano*, 2019, **6**, 3638–3652.
- S. Pu, C. Yan, H. Huang, S. Liu and D. Deng, Toxicity of nano-CuO particles to maize and microbial community largely depends on its bioavailable fractions, *Environ. Pollut.*, 2019, **255**, 113248.
- X. Gao, A. Avellan, S. Laughton, R. Vaidya, S. M. Rodrigues, E. A. Casman and G. V. Lowry, CuO nanoparticle dissolution and toxicity to wheat (*Triticum aestivum*) in rhizosphere soil, *Environ. Sci. Technol.*, 2018, **52**, 2888–2897.
- J. R. Velicogna, D. M. Schwertfeger, C. Beer, A. H. Jesmer, J. Kuo, H. Chen, R. P. Scroggins and J. I. Princz, Phytotoxicity of copper oxide nanoparticles in soil with and without biosolid amendment, *NanoImpact*, 2020, **17**, 100196.
- H. Qiu and E. Smolders, Nanospecific phytotoxicity of CuO nanoparticles in soils disappeared when bioavailability factors were considered, *Environ. Sci. Technol.*, 2017, **51**, 11976–11985.
- H. Shang, H. Guo, C. Ma, C. Li, B. Chefetz, T. Polubesova and B. Xing, Maize (*Zea mays* L.) root exudates modify the surface chemistry of CuO nanoparticles: Altered aggregation, dissolution and toxicity, *Sci. Total Environ.*, 2019, **690**, 502–510.
- M. Wu, X. Wang, Z. Jia, K. De Schamphelaere, D. Ji, X. Li and X. Chen, Modeling acute toxicity of metal mixtures to wheat (*Triticum aestivum* L.) using the biotic ligand model-based toxic units method, *Sci. Rep.*, 2017, **7**, 9443.
- D. R. Parker, J. F. Pedler, Z. A. S. Ahnstrom and M. Resketo, Reevaluating the free-ion activity model of trace metal toxicity toward higher plants: Experimental evidence with copper and zinc, *Environ. Toxicol. Chem.*, 2001, **20**, 899–906.
- S. K. Misra, A. Dybowska, D. Berhanu, S. N. Luoma and E. Valsami-Jones, The complexity of nanoparticle dissolution and its importance in nanotoxicological studies, *Sci. Total Environ.*, 2012, **438**, 225–232.
- D. A. Palmer, The solubility of crystalline cupric oxide in aqueous solution from 25 °C to 400 °C, *J. Chem. Thermodyn.*, 2017, **114**, 122–134.
- C. Peng, C. Shen, S. Zheng, W. Yang, H. Hu, J. Liu and J. Shi, Transformation of CuO nanoparticles in the aquatic environment: Influence of pH, electrolytes, and natural organic matter, *Nanomaterials*, 2017, **7**, 326.
- Z. Y. Wang, A. von dem Bussche, P. K. Kabadi, A. B. Kane and R. H. Hurt, Biological and environmental transformations of Cu-based nanomaterials, *ACS Nano*, 2013, **7**, 8715–8727.
- C. Gunawan, W. Y. Teoh, C. P. Marquis and R. Amal, Cytotoxic origin of Cu(II) oxide nanoparticles: Comparative studies with micron-sized particles, leachate, and metal salts, *ACS Nano*, 2011, **5**, 7214–7225.
- C. Peng, H. Tong, P. Yuan, L. Sun, L. Jiang and J. Shi, Aggregation, sedimentation and dissolution of copper oxide nanoparticles: Influence of low-molecular-weight organic acids from root exudates, *Nanomaterials*, 2019, **9**, 841.
- P. McManus, J. Hortin, A. J. Anderson, A. R. Jacobson, D. W. Britt, J. Stewart and J. E. McLean, Rhizosphere interactions between copper oxide nanoparticles and wheat root exudates

- in a sand matrix: Influences on copper bioavailability and uptake, *Environ. Toxicol.*, 2018, **37**, 2619–2632.
- 20 C. Peng, H. Zhang, H. X. Fang, C. Xu, H. M. Huang, Y. Wang, L. J. Sun, X. F. Yuan, Y. X. Chen and J. Y. Shi, Natural organic matter-induced alleviation of the phytotoxicity to rice (*Oryza sativa* L.) caused by Cu oxide nanoparticles, *Environ. Toxicol. Chem.*, 2015, **34**, 1996–2003.
 - 21 C. Jiang, B. T. Castellon, C. W. Matson, G. R. Aiken and H. Hsu-Kim, Relative contributions of Cu oxide nanoparticles and dissolved Cu to Cu uptake kinetics of Gulf Killifish (*Fundulus grandis*) embryos, *Environ. Sci. Technol.*, 2017, **51**, 1395–1404.
 - 22 J. R. Conway, A. S. Adeleye, J. Gardea-Torresdey and A. A. Keller, Aggregation, dissolution, and transformation of Cu nanoparticles in natural waters, *Environ. Sci. Technol.*, 2015, **49**, 2749–2756.
 - 23 J. Zhao, Z. Y. Wang, Y. H. Dai and B. S. Xing, Mitigation of CuO nanoparticle-induced bacterial membrane damage by dissolved organic matter, *Water Res.*, 2013, **47**, 4169–4178.
 - 24 A. Pradhan, P. Gerald, S. Seena, C. Pascoal and F. Cássio, Humic acid can mitigate the toxicity of small copper oxide nanoparticles to microbial decomposers and leaf decomposition in streams, *Freshwater Biol.*, 2016, **61**, 2197–2210.
 - 25 D. F. C. Morris and E. L. Short, Stability constants of Cu (II) chloride complexes, *J. Chem. Soc.*, 1962, 2672–2675.
 - 26 H. Bilinski, R. Huston and W. Stumm, Determination of the stability constants of some hydroxo and carbonate complexes of Pb(II), Cu(II), Cd(II) and Zn(II) in dilute solutions by anodic stripping voltammetry and differential pulse polarography, *Anal. Chim. Acta*, 1976, **84**, 157–164.
 - 27 J. Buekers, L. Van Laer, F. Amery, S. Van Buggenhout, A. Maes and E. Smolders, Role of soil constituents in fixation of soluble Zn, Cu, Ni, and Cd added to soils, *Eur. J. Soil Sci.*, 2007, **58**, 1514–1524.
 - 28 S. R. Smith, Effect of soil pH on availability to crops of metals in sewage sludge-treated soils. I. Nickel, copper, and zinc uptake and toxicity to ryegrass, *Environ. Pollut.*, 1994, **85**, 321–327.
 - 29 R. L. Blevins and H. F. Massey, Evaluation of two methods of measuring available soil copper and the effects of soil pH and extractable aluminum on copper uptake by plants, *Soil Sci. Soc. Am. J.*, 1959, **23**, 296–298.
 - 30 Y. Lin, H. S. Allen and D. M. di Toro, Validation of Cu toxicity to barley root elongation in soil with the Terrestrial Biotic Ligand Model developed from sand culture, *Ecotoxicol. Environ. Saf.*, 2018, **148**, 336–345.
 - 31 A. S. Adeleye, J. R. Conway, T. Perez, P. Rutten and A. A. Keller, Influence of extracellular polymeric substances on the long-term fate, dissolution, and speciation of copper-based nanoparticles, *Environ. Sci. Technol.*, 2014, **48**, 12561–12568.
 - 32 L. Z. Miao, C. Wang, J. Hou, P. F. Wang, Y. H. Ao, Y. Li, B. W. Lv, Y. Y. Yang, G. X. You and Y. Xu, Enhanced stability and dissolution of CuO nanoparticles by extracellular polymeric substances in aqueous environment, *J. Nanopart. Res.*, 2015, **17**, 404.
 - 33 C. O. Dimkpa, J. E. McLean, D. W. Britt and A. J. Anderson, CuO and ZnO nanoparticles differently affect the secretion of fluorescent siderophores in the beneficial root colonizer, *Pseudomonas chlororaphis* O6, *Nanotoxicology*, 2012, **6**, 635–642.
 - 34 C. O. Dimkpa, J. E. McLean, D. W. Britt, W. P. Johnson, B. Arey, A. S. Lea and A. J. Anderson, Nanospecific inhibition of pyoverdine siderophore production in *Pseudomonas chlororaphis* O6 by CuO nanoparticles, *Chem. Res. Toxicol.*, 2012, **25**, 1066–1074.
 - 35 X. Gao, S. M. Rodrigues, E. Spielman-Sun, S. Lopes, S. Rodrigues, Y. Zhang, A. Avellan, R. M. B. O. Duarte, A. Duarte, E. A. Casman and G. V. Lowry, Effect of soil organic matter, soil pH, and moisture content on solubility and dissolution rate of CuO NPs in soil, *Environ. Sci. Technol.*, 2019, **53**, 4959–4967.
 - 36 X. Gao, E. Spielman-Sun, S. M. Rodrigues, E. A. Casman and G. V. Lowry, Time and nanoparticle concentration affect the extractability of Cu from CuO NP-amended soil, *Environ. Sci. Technol.*, 2017, **51**, 2226–2234.
 - 37 APHA, in *Standard methods for the examination of water and wastewater*, American Public Health Association, Washington, D. C., 22nd edn, 2012.
 - 38 C. O. Dimkpa, U. Singh, P. S. Bindraban, W. H. Elmer, J. L. Gardea-Torresdey and J. C. White, Zinc oxide nanoparticles alleviate drought-induced alterations in sorghum performance, nutrient acquisition, and grain fortification, *Sci. Total Environ.*, 2019, **688**, 926–934.
 - 39 J. D. Rhoades, in *Methods of soil analysis: Part 3-chemical methods*, Soil Science Society of America, Inc. & American Society of Agronomy, Inc., Madison, WI, 1996, ch. 14, pp. 417–435.
 - 40 A. Jacobson, S. Doxey, M. Potter, J. Adams, D. Britt, P. McManus, J. McLean and A. Anderson, Interactions between a plant probiotic and nanoparticles on plant responses related to drought tolerance, *Ind. Biotechnol.*, 2018, **14**, 148–156.
 - 41 J. B. Jones and V. W. Case, in *Soil Testing and Plant Analysis*, American Society of Agronomy, Madison, WI, 1990.
 - 42 R. Campisano, K. Hall, J. Griggs, S. Willison, S. Reimer, H. Mash, M. Magnuson, L. Boczek and E. Rhodes, *Selected Analytical Methods for Environmental Remediation and Recovery (SAM) 2017*, U.S. Environmental Protection Agency, Washington, D.C., 2017.
 - 43 J. Rachou, C. Gagnon and S. Sauve, Use of an ion-selective electrode for free copper measurements in low salinity and low ionic strength matrices, *Environ. Chem.*, 2007, **4**, 90–97.
 - 44 Merck KGaA, *User guide: Amicon® Ultra-4 centrifugal filter devices*, Darmstadt, Germany, 2018.
 - 45 C. M. H. Ferreira, I. S. S. Pinto, E. V. Soares and H. M. V. M. Soares, (Un)suitability of the use of pH buffers in biological, biochemical, and environmental studies and their interaction with metal ions – a review, *RSC Adv.*, 2015, **5**, 30989–31003.
 - 46 SAS Institute, Inc., *JMP*, version 8.0.2, Cary, North Carolina, 2009.

- 47 B. Ravel, *Athena*, version 0.9.25, 2016.
- 48 B. Ravel, *[Iffeffit] meaning of linear combination fit reports*, <http://millenia.cars.aps.anl.gov/pipermail/iffeffit/2014-August/007520.html>, (accessed November 2018).
- 49 R Foundation for Statistical Computing, *R*, version 3.2.2, 2015.
- 50 J. P. Gustaffson, *Visual MINTEQ*, version 3.1, KTH, Stockholm, Sweden, 2013.
- 51 J. Leitner, D. Sedmidubský and O. Jankovský, Size and shape-dependent solubility of CuO nanostructures, *Materials*, 2019, **12**, 3355.
- 52 R. D. Kent and P. J. Vikesland, Dissolution and persistence of copper-based nanomaterials in undersaturated solutions with respect to cupric solid phases, *Environ. Sci. Technol.*, 2016, **50**, 6772–6781.
- 53 C. Chen, X. Chen, Y. Yang, A. G. Hay, X. Yu and Y. Chen, Sorption and distribution of copper in unsaturated *Pseudomonas putida* CZ1 biofilms as determined by X-ray fluorescence microscopy, *Appl. Environ. Microbiol.*, 2011, **77**, 4719–4727.
- 54 C. A. Van Kirk and K. Raschke, Presence of chloride reduces malate production in epidermis during stomatal opening, *Plant Physiol.*, 1978, **61**, 361–364.
- 55 B. E. Vencalek, S. N. Laughton, E. Spielman-Sun, S. M. Rodrigues, J. M. Unrine, G. V. Lowry and K. B. Gregory, *In situ* measurement of CuO and Cu(OH)₂ nanoparticle dissolution rates in quiescent freshwater mesocosms, *Environ. Sci. Technol. Lett.*, 2016, **3**, 375–380.
- 56 J. Zhao, G. Chu, B. Pan, B. Y. Zhou, M. Wu, Y. Liu, W. Duan, D. Lang, Q. Zhao and B. Xing, Homo-conjugation of low molecular weight organic acids competes with their complexation with Cu(II), *Environ. Sci. Technol.*, 2018, **52**, 5173–5181.
- 57 S. Klitzke, G. Metreveli, A. Peters, G. E. Schaumann and F. Lang, The fate of silver nanoparticles in soil solution - sorption of solutes and aggregation, *Sci. Total Environ.*, 2015, **535**, 54–60.
- 58 L. Wang, N. Habibul, D. He, W. Li, X. Zhang, H. Jiang and H. Yu, Cu release from Cu nanoparticles in the presence of natural organic matter, *Water Res.*, 2015, **68**, 12–23.
- 59 W. Chen, N. Habibul, X. Liu, G. Sheng and H. Yu, FTIR and synchronous fluorescence heterospectral two-dimensional correlation analyses on the binding characteristics of Cu onto dissolved organic matter, *Environ. Sci. Technol.*, 2015, **49**, 2052–2058.
- 60 R. M. Silverstein, G. C. Bassler and T. C. Morrill, in *Spectrometric identification of organic compounds*, John Wiley & Sons, New York, 1963, pp. 83–139.
- 61 Y. Wang, W. Liu, R. Li and Y. Zhang, New insight into chemical changes between dissolved organic matter and environmental nano-CuO pollutants binding experiment using multi-spectroscopic techniques, *J. Mol. Liq.*, 2019, **291**, 111278.
- 62 K. Akeyama, H. Kuroda and N. Kosugi, Cu K-edge XANES and electronic structure of trivalent, divalent, and monovalent Cu oxides, *Jpn. J. Appl. Phys.*, 1993, **32**, 98–100.
- 63 R. Sekine, E. R. Marzouk, M. Khaksar, K. G. Scheckel, J. P. Stegemeier, G. V. Lowry, E. Donner and E. Lombi, Aging of dissolved copper and copper-based nanoparticles in five different soils: Short-term kinetics vs. long-term fate, *J. Environ. Qual.*, 2017, **46**, 1198–1205.